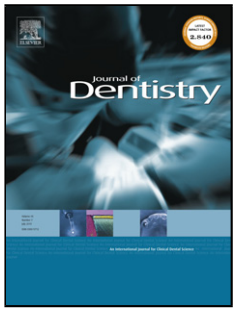

Title: Biofilm formation and release of fluoride from dental restorative materials in relation to their surface properties

Authors: Sebastian Hahnel, Andrei C. Ionescu, Gloria Cazzaniga, Marco Ottobelli, Eugenio Brambilla

PII: S0300-5712(17)30033-7
DOI: http://dx.doi.org/doi:10.1016/j.jdent.2017.02.005
Reference: JJOD 2734

To appear in: *Journal of Dentistry*

Received date: 18-12-2016
Revised date: 6-2-2017
Accepted date: 11-2-2017

Please cite this article as: {http://dx.doi.org/

<AT>Biofilm formation and release of fluoride from dental restorative materials in relation to their surface properties
Biofilm on restorative materials

<AU>Sebastian Hahnel DDS[a*] ##Email##sebastian.hahnel@ukr.de##/Email##, Andrei C. Ionescu DDS, PhD[b], Gloria Cazzaniga DDS[b], Marco Ottobelli DDS[b], Eugenio Brambilla DDS[b]
<AU>

<AFF>[a]Department of Prosthetic Dentistry, Regensburg University Medical Center, Regensburg, Germany
<AFF>[b]Department of Biomedical, Surgical and Dental Sciences, IRCCS Galeazzi Institute, University of Milan, Italy

<PA>Sebastian Hahnel (DDS) Department of Prosthetic Dentistry Regensburg University Medical Center 93042 Regensburg Germany Tel.: +49-941-9446059 Fax: +49-941-9446171.

<ABS-HEAD>Abstract

<ABS-P><ST>Objectives</ST> To elucidate the impact of surface properties and the release of fluoride from different glass ionomer cements on biofilm formation.

<ABS-P>

<ABS-P><ST>Methods</ST> Standardized specimens manufactured from various classes of glass ionomer cements (GICs), a resin-based composite (RBC), and human enamel were subjected to surface analyses. Subsequent to simulation of salivary pellicle formation, *Streptococcus mutans* biofilm formation was initiated using a drip flow reactor for 48 h and 96 h. Biofilms were characterized by determining viable bacterial biomass and 3D biofilm architecture using SEM and CLSM; the release of fluoride from the specimens was measured using the ion selective micro method in dependence on various experimental conditions (incubation with sterile broth/bacteria/acid).
<ABS-P><ST>Results</ST> Surface properties and biofilm formation correlated poorly, while the release of fluoride correlated well with viable streptococcal biomass and SEM/CLSM analyses. For all investigated materials, biofilm formation was lower than on enamel. The release of fluoride showed a significant dependency on the experimental conditions applied; the presence of biofilms reduced fluoride release in comparison to sterile incubation conditions.
<ABS-P><ST>Conclusions</ST> Within the limitations of a laboratory study, the results suggest that biofilm formation on GICs cannot be easily predicted as a function of substratum surface parameters. The release of fluoride from glass ionomer cements contributes to control biofilm formation particularly in its early phases.
<ABS-P>*Clinical Significance:* Glass ionomer cements can actively control microbial biofilm formation, while biofilms modulate the release of fluoride from GIC materials.

<KWD>Keywords: *biofilm*; *fluoride*; *glass ionomer cement*; *resin composite*; *Streptococcus mutans*

Introduction

Glass ionomer cements (GICs) have been introduced in dentistry in the mid-seventies [1], featuring some favourable properties such as a chemical bond to enamel and dentin, a coefficient of thermal expansion almost equal to natural tooth tissues, and the ability to release fluoride over a significant amount of time [2,3]. As a result, GICs are considered as biomaterials that may prevent [3,5] and inactivate [6,7] dental caries and its progression. While early glass ionomer cement formulations featured poor mechanical properties, the recently introduced high-viscosity GICs (HV-GICs) featured significantly improved hardness and stress resistance in comparison to early and conventional GICs. In addition to their application as restorative materials, GICs can successfully be used for cementation of indirect restorations [8].

As secondary caries remains one of the most frequent reasons for failure of dental restorations [9,10], it has often been highlighted that biofilm formation on the surface of dental restorative materials may contribute to the establishment of secondary caries lesions. In GIC restorations, the fluoride released by GICs may serve as a buffer that neutralizes acids secreted by oral bacteria and may inhibit the growth of cariogenic microorganisms [11,12]. Recent studies have highlighted a correlation between the release of fluoride from GICs and the properties of *Streptococcus mutans* biofilms on their surface, suggesting that acidogenicity, dry weight, the amount of extracellular polysaccharides (EPS), as well as biovolumes and EPS thickness are significantly reduced in biofilms on the surface of GICs which feature a high release of fluoride [13]. Employing a clinical approach for the analysis of biofilm formation, other researchers pointed out that despite of lacking significant differences in biofilm formation between various materials such as GICs, amalgam, resin-based composite, and ceramic, there was a tendency towards a lower number of viable bacterial cells in biofilms grown on restorations made of GICs and amalgam [14]. Similar results have been published by other groups [15], while some researchers suggested that biofilm formation is not necessarily reduced on fluoride-releasing GICs [16,17]. Thus, the aim of the present laboratory study was to elucidate the impact of surface properties and the release of fluoride from various classes of GICs on *Streptococcus mutans* biofilm formation in dependency on incubation times. The study hypotheses were that (I) *Streptococcus mutans* biofilm formation is not affected by the release of fluoride, (II) the release of fluoride is not influenced by the incubation time, and (III) the release of fluoride is not influenced by exposure of GIC surfaces to biofilms.

Materials and Method

Specimen preparation

Standardized specimens were prepared from an experimental light-curing glass ionomer cement (resin-modified GIC; A), a compomer (*Glasiosite*; B), a luting GIC (*Meron*; C), a high viscosity GIC (*Ionostar plus*; D), and from a reference nanohybrid resin-based composite (RBC, *Grandioso*; E, all by VOCO GmbH, Cuxhaven, G). For preparation of a single specimen, a standardized amount of each material was placed into a custom made steel mould with a diameter of 6.0 mm and a height of 2.0 mm, condensed against a glass plate and covered with a cellulose acetate strip (Mylar®) until cured. Compomer, resin-modified GIC, and RBC specimens were light-cured in direct contact for 40 s using a hand-held light curing unit (LCU; SDI Radii plus, SDI, Bayswater, AUS; 1500 mW/cm^2). A total of 83 specimens for each material were produced. The specimens were then subjected to a standardized polishing protocol, including polishing with 1000/4000-grit grinding paper (Buehler, Lake Bluff, IL, USA) using a polishing machine (Motopol 8; Buehler, Düsseldorf, G). Anterior human teeth extracted for clinical reasons were obtained from the Oral Surgery Unit at the Department of Biomedical, Surgical and Dental Sciences (Milan, Italy). A total of 83 round enamel-dentin slabs with a diameter of 6.0 mm and a thickness of 2.0 mm were cut from the labial surfaces using a water-cooled trephine diamond bur (INDIAM, Carrara, I). Dentin bottoms were removed, and the enamel surfaces (enamel, E) were polished as described for the dental materials above. All specimens were subsequently stored under light-proof conditions in artificial saliva for six days at 37±1°C prior to the further experiments to allow for maturation of the cement, to eliminate potential impacts of a fluoride burst and,

for the resin-modified GIC, the compomer, and RBC, to minimize the impact of residual monomer leakage on cell viability. The artificial saliva used in the present study allows a reproduction of the average electrolytic composition of human whole saliva and was prepared by mixing 100 mL of 150 mM $KHCO_3$, 100 mL of 100 mM NaCl, 100 mL of 25 mM K_2HPO_4, 100 mL of 24 mM Na_2HPO_4, 100 mL of 15 mM $CaCl_2$, 100mL of 1,5 mM $MgCl_2$, and 6 mL of 25mM citric acid. The volume was made up to 1 L and the pH was adjusted to 7.0 by pipetting NaOH 4M or HCl 4M solutions under vigorous stirring. All specimens undergoing surface analysis were subsequently cleaned using distilled water and applicator brush tips (3M ESPE, Seefeld, G).

Surface analysis

Surface roughness

Peak-to-valley surface roughness (R_a) was determined on five randomly selected specimens for each group material using a profilometric contact surface measurement device (Perthen S6P, Feinprüf-Perthen, Göttingen, G). A distance of 1.75 mm was measured in three randomly selected line scans perpendicular to the expected grinding grooves using a standard diamond tip (tip radius 2 µm, tip angle 90°) and a cut off level of 0.25.

Surface free energy

Contact angles between the surface of the various materials and three liquids differing in hydrophobicity (bidistilled water, diiodomethane, ethylene glycol) were determined using the sessile drop method and a computer-aided contact angle measurement device (OCA 15plus, DataPhysics Instruments GmbH, Filderstadt, G). A total of eight drops for each liquid (drop volume 0.2 µL) were analyzed on each of four randomly selected specimens for each material. Left and right contact angles were averaged and the surface free energy was calculated according to the approach introduced by Owens and Wendt [18].

Energy-dispersive X-ray Spectroscopy (EDS)

Two randomly selected specimens for each material were subjected to EDS surface analysis. A scanning electron microscope coupled with an EDS probe (EDAX Genesis 2000, Ametek GmbH, Meerbusch, G) was used to acquire full frames of the surfaces of the specimens employing an accelerating voltage of 20 kV, a magnification of 2000x and an acquisition time of 200 s.

Microbiological procedures

Saliva preparation

Stimulated whole saliva was collected by expectoration from three healthy donors in accordance with the protocol published by Guggenheim et al. [19]. Saliva was collected in chilled tubes, pooled, heated to 60°C for 30 min to inactivate endogenous enzymes, and was then centrifuged (12.000xg) for 15 min at 4°C. The supernatant was transferred into sterile tubes, stored at -20°C, and thawed at 37°C for 1 h directly prior to the experiments.

Bacteria

Streptococcus mutans ATCC 35668 was cultured according to a previously published protocol [20]. Briefly, Mitis Salivarius Bacitracin agar inoculated plates were incubated for 48 h at 37 °C in a 5% supplemented CO_2 environment. A total of 1% sucrose was added to a pure suspension of the microorganism in Brain Heart Infusion obtained from these plates after an incubation of 12 h at 37 °C in a 5% supplemented CO_2 environment. *S. mutans* cells were harvested by centrifugation (2200 rpm, 19 °C, 5 min), washed twice with phosphate-buffered saline (PBS), and resuspended. The suspension was subsequently subjected to low intensity ultrasonic energy (Sonifier model B-150; Branson, Danbury, CT, USA; operating at 7-W energy output for 30 s) in order to disperse bacterial chains. The suspension was then adjusted to a value of 1.0 on the McFarland scale, corresponding to a microbial concentration of approximately 3.0×10^8 cells/mL.

Biofilm formation

The drip-flow reactor (M-DFR) employed in the present study was a modification of a commercially available Drip Flow Reactor (DFR 110; BioSurface Technologies, Bozeman, MT, USA). The modified design allowed the placement of customized specimen-trays on the bottom of the flow cells and the complete immersion of the surfaces of the specimens into the surrounding flowing medium [21]. A total of 72 randomly selected specimens for each material were placed in Teflon trays, which fixed the specimens tightly and exposed their surfaces to the surrounding medium; the trays were fixed on the bottom of each flow cell of the M-DFR. All tubing and specimen-containing trays were sterilized prior to the experiments using a chemiclave with hydrogen peroxide gas plasma technology (Sterrad; ASP, Irvine, CA, USA). By limiting the maximum temperature to 45°C, heat-related damage of the specimens was avoided. The whole M-DFR was assembled inside a sterile hood and transferred into a thermostat in order to operate under a standardized temperature of 37°C. For simulation of salivary pellicle formation, the surfaces of the specimens in each flow cell were exposed to thawed sterile saliva for 24 h. Subsequently, excess saliva was discarded. *S. mutans* monospecific biofilm development was obtained on the surfaces of the specimens by inoculating 10 mL of *S. mutans* suspension into each flow cell.
A total of 40 specimens for each material were inoculated with *S. mutans* suspension, 16 specimens were incubated under sterile conditions and 16 additional specimens were incubated under acidic conditions (pH=4.0) generated by a flow of buffered lactic acid/potassium lactate solution. After 4 h, a multichannel, computer-controlled peristaltic pump (RP-1; Rainin, Emeryville, CA, USA) was turned on to provide a constant flow of nutrient broth through the flow cells. The sterile nutrient broth was enriched with 10.0 g/L sucrose and consisted of 2.5 g/L mucin (type II, porcine gastric), 2.0 g/L bacteriological peptone, 2.0 g/L tryptone, 1.0 g/L yeast extract, 0.35 g/L NaCl, 0.2 g/L KCl, 0.2 g/L CaCl2, 0.1 g/L cysteine hydrochloride, 0.001 g/L hemin, and 0.0002 g/L vitamin K1. The flow rate was set to 9.6 ml/h [19].

MTT assay

Viable biomass adherent to the surfaces was assessed after either 48 h (n=8) or 96 h (n=8) incubation period using a MTT-based assay [21]. In brief, MTT stock solution was prepared by dissolving 5 mg/mL 3-(4,5)-dimethylthiazol-2-yl-2,5-diphenyltetrazolium bromide in sterile PBS; PMS stock solution was prepared by dissolving 0.3 mg/mL of N-methylphenazinium methyl sulphate in sterile PBS. The solutions were stored at 2°C in light-proof vials until the day of the experiment, when a fresh measurement solution (FMS) was prepared by diluting 1:10 v/v of MTT stock solution and 1:10 v/v of PMS stock solution in sterile PBS. A lysing solution (LS) was prepared by dissolving 10% v/v of sodium dodecyl sulphate and 50% v/v dimethylformamide in deionized water.
After either 48 h or 96 h of incubation in the M-DFR, the flow of nutrient broth was stopped, the flow cells were opened, and the trays containing the specimens were carefully removed and immediately placed in dishes containing sterile PBS at 37°C. The specimens were subsequently gently removed from the tray, passed into another dish with sterile PBS at 37°C in order to remove non-adhered cells, and finally transferred into 48-well plates. 300 µl of FMS solution were added to each well, and the plates were incubated for 3 h at 37°C under light-proof conditions.
During incubation, electron transport across the microbial plasma membrane and, to a lesser extent, microbial redox systems convert the yellow salt to insoluble purple formazan crystals. The conversion at the cell membrane level was facilitated by the intermediate electron acceptor (PMS). The unreacted FMS solution was gently removed and the formazan crystals were dissolved by adding 300 µL of LS to each well. The plates were stored for an additional 1 h under light-proof conditions at room temperature; 100 µL of the solution were then transferred into the wells of 96-well plates. The absorbance of the solution was measured using a spectrophotometer (Genesys 10-S, Thermo Spectronic, Rochester, NY, USA) at a wavelength of 550 nm; results were expressed as relative absorbance in optical density (OD) units corresponding to the amount of adherent, viable and metabolically active biomass.

Confocal laser-scanning microscopy

A total of four specimens (48 h incubation, n=2; 96 h incubation, n=2) were gently removed from the flow cells, rinsed twice with sterile PBS, and stained using the FilmTracer™ LIVE/DEAD® Biofilm Viability Kit (Invitrogen Ltd., Paisley, UK). Stained biofilms were analyzed using confocal laser-scanning microscopy (Leica TCS SP2, Leica Microsystems, Wetzlar, G) immediately after the staining procedures. Four randomly selected image stack sections were recorded for each specimen and incubation time. Confocal images were obtained using a dry 20x (NA = 0.7) objective and digitalized using the Leica Application Suite Advanced Fluorescence Software (LAS-AF, Leica microsystems) at a resolution of 2048x2048 pixels with a zoom factor of 1.0 at a scan speed of 400 Hz. Three channels were acquired: one was excited at 405 nm and observed at 420-470 nm in order to digitally subtract in post-processing the specimens´ autofluorescence signal whenever present; the other two channels were excited at a wavelength of 488 nm. Emission was acquired at 500-570 nm (green channel, live bacteria) and 610-760 nm (red channel, dead bacteria). For each image stack section, 3D-rendering reconstructions were obtained using ImageJ (National Institutes of Health, Bethesda, MD, USA), and Drishti (Ajay Limaye, Australian National University, CAN, AUS http://sf.anu.edu.au/Vizlab/drishti/) was used for 3D reconstructions.

Scanning electron microscopy

A total of four specimens (48 h incubation, n=2; 96 h incubation, n=2) were gently removed from the flow cells, rinsed twice with sterile PBS, and placed into a cacodylate-buffered 2% glutaraldehyde–fixative solution (pH=7.4) for 48 h. The specimens were then passed through a graded ethanol series (50, 70, 80, 85, 90, 95, and 100%, v/v). Finally, the specimens were subjected to critical point drying (Critical-Point Dryer, EMS 850, Hatfield, PA, USA), mounted on stubs with conductive glue, sputter coated (JEOL FFC-1100, Japan), and analyzed with a scanning electron microscope (JEOL JSM-5300, Japan) at a magnification of 500x–5000x. Four randomly selected fields (2000x) were recorded for each specimen.

Determination of the release of fluoride

The release of fluoride from each material was determined for specimens subjected to biofilm formation (G1; 48 h (n=8) or 96 h (n=8)) for specimens kept under sterile flow conditions (G2; 48 h (n=8) or 96 h (n=8)), and for specimens kept under the acidic buffered solution flow (G3; 48 h (n=8) or 96 h (n=8)). The latter condition simulated a continuous acidic environment as expected in biofilms with low pH value. Specimens were removed from the flow cells and adherent biomass (for group G1 only) was detached by sonication in distilled water in an ultrasonic bath for 5 min. The specimens (G1, G2, and G3) were immersed into 400 µL of fresh artificial saliva and the cumulative concentration of fluoride in the supernatant was determined after a period of seven days using the ion-selective electrode micro method as described previously [22]. In brief, a stock solution with a fluoride concentration of 1000 ppm was appropriately diluted with artificial saliva to obtain fluoride standards with fluoride concentrations ranging from 0.0019 to 64 parts per million (ppm). A calibration curve was obtained by measuring fluoride standards using a digital pH/mV meter (SA-720, Orion Research Inc, Boston, MA, USA). Sodium acetate buffer 20% v/v with EDTA as ionic strength adjustor was added to each standard prior to analysis. A negative standard (0 ppm fluoride) was prepared by adding 20% v/v of sodium acetate buffer with EDTA to artificial saliva; this solution was also used to rinse the electrodes between the single measurements.

Statistical analysis

Statistical analyses were performed using JMP 10.0 software (SAS Institute, Cary, NC, USA). Normal distribution of data was checked using Shapiro-Wilk's test and homogeneity of variances was verified using Levene's test. Means and standard errors were calculated from the raw data. One-way analysis of variance (ANOVA) was employed to analyze data gathered for surface characterization. Biofilm formation (MTT assay) was analysed using two-way ANOVA setting material and incubation time as fixed factors. Release of fluoride was statistically examined using three-way ANOVA setting material, incubation time, and incubation mode as fixed factors. Tukey HSD test was employed for post-hoc analysis ($p<0.05$).

Results

Surface analysis

One-way ANOVA indicated significant differences in surface roughness between the various materials (P<.001). Significantly lowest surface roughness was identified for B, E, and F, while significantly higher surface roughness was identified for A, C, D (P<.001) (Figure 1). With regard to surface free energy, one-way ANOVA identified no significant differences in total surface free energy (P=.999) or in its polar (P=.965) and disperse (P=.815) contributions (Figure 2).

EDS analyses (Table 1) indicated the presence of a relatively high amount of fluoride on the surface of A, C, and B, with values ranging between approximately 8.5 and 10.5 % wt. Levels of fluoride decreased significantly from baseline after incubation with bacteria or sterile conditions (Table 2).

Biofilm formation (Figure 3)

Two-way ANOVA indicated significant differences in relative absorbance values between the various materials and incubation times (P<.001, each), indicating significant differences in biofilm formation. A significant interaction effect was identified between the two fixed factors (P<.001), indicating that biofilm formation varied on the tested materials surfaces in dependence of the incubation time. After 48 h, post-hoc analyses demonstrated lowest absorbance values for C and D; highest values were identified for F. Intermediate absorbance values were identified for E, A, and B. After 96 h, generally less pronounced differences in absorbance values were identified. However, post-hoc analyses identified significantly lowest values for C and the D, and highest values for F.

Release of fluoride (Figure 4)

Three-way analysis of variance indicated significant differences in the release of fluoride, suggesting a significant impact of incubation times, material, and the presence of biofilms (P<.0001). Significant interaction effects were observed between all fixed factors, suggesting that different materials feature different fluoride kinetics and that the presence of biofilms has a significant impact on the release of fluoride. Increasing incubation time coincide with a significant decrease in the release of fluoride from C and D when incubated either with or without bacteria, and from A when incubated with bacteria (P=.004 for C and D, P=.0282 for A). The presence of biofilms on the surface of the specimens significantly enhanced the amount of fluoride detected after the various incubation times (P<.001 for A, C and D, comparing biofilm incubation with both incubation under sterile and acidic conditions.). Relevant amounts of released fluoride (means ± 1 SD) were overall identified for A (11.83±4.65), C (16.56 ± 7.72), and D (18.46 ± 9.08), while no relevant relevant release of fluoride was measured for B (1.2 ± 1.03), E (0.19 ± 0.16), and F (0.33 ± 0.35).

Confocal laser scanning microscopy

After 48 h (Figure 5), the presence of mature, multilayered biofilm structures was observed on the various materials. F was completely covered by a uniform layer of mature biofilm, which completely canopied the surface and formed isolated thick and compact structures. For E, a similar biofilm pattern as in F was identified, yet a slightly higher prevalence of microcolonies formed by dead bacteria was observed. The biofilms on the other materials were represented by isolated, compact microcolonies with voids in between. Biofilms on A and B showed predominantly viable microcolonies in the peripher areas of the colony and dead microcolonies in the central areas parts. In biofilms on C and D, microcolonies featuring a high ratio of dead to viable bacteria that were predominantly located adjacent to the substratum surfaces were identified.

After 96 h (Figure 6), the surfaces of all materials were covered by microcolonies characterized by confluent growth. The surfaces of the materials E and F were completely

canopied by confluent biofilm structures featuring an increased thickness and complexity in comparison to their 48 h counterparts; however, a higher ratio of dead to viable bacterial cells was identified. In all biofilms on all other materials, the biofilms were characterized by evenly spaced confluent microcolonies. In biofilms on the materials A and B, prevalently viable microcolonies were identified, while biofilms on the materials C and D were very similar to their counterparts after an incubation time of 48 h.

Scanning electron microscopy

After 48 h (Figure 7), the presence of mature, multilayered biofilm structures embedded in extracellular matrix (EPS) was observed on all materials. The surface of F was completely covered by a uniform layer of mature biofilm. In all materials, the surface of the substratum material surface could still be identified. Less biofilm formation could be observed on the surfaces of C, D, and – to a lesser extent – B, compared to the other materials. On B and E, higher amounts of extracellular matrix were identified than on the other materials.

After 96 h (Figure 8), the surfaces of all materials were completely covered with a uniform layer of mature biofilm embedded into its matrix. In its peripheral areas, the biofilms showed chain-shaped, actively replicating bacterial cells. The substratum surface was still visible in some areas on the materials C and – to a lesser extent – D, suggesting that the cell density was lower in biofilms on these materials. A higher amount of extracellular matrix could be identified for biofilms on A, B, and E in comparison to the other materials.

Discussion

The results of the present laboratory study did not indicate a simple relationship between substratum surface properties and biofilm formation on the tested materials, and underline that *Streptococcus mutans* biofilm formation is significantly affected by the release of fluoride.

Regarding the first study hypothesis, a tendency towards reduced biofilm formation on fluoride releasing GICs was identified, yet statistical analyses indicated that *S. mutans* biofilm formation was not necessarily lower on materials with a high release of fluoride in comparison to those featuring lower or no release of fluoride. For both incubation times, highest biofilm formation was observed on enamel, while lowest values were identified for the luting GIC and the HV-GIC; these materials as well as the light-curing GIC released significantly higher levels of fluoride than any other material. However, despite of the lacking release of fluoride, biofilm formation on the compomer and RBC was at least similar to the light-curing GIC. These observations indicate that the release of fluoride is not the only parameter determining biofilm formation on the surface of these materials, and partially disagree with the results published by other groups, who identified a correlation between the release of fluoride, biofilm dry weight, and the presence of water-insoluble extracellular polysaccharides in biofilms on various GICs [13]. It is well known that fluoride is able to impair *S. mutans* acid production by inhibiting the bacterial enzyme ATPase that is in charge for maintaining the intracellular pH. Also, aluminum ions released from the GICs may significantly enhance the ATPase-inhibiting activity of fluoride [23]. Moreover, it has been reported that the glycolytic enzyme enolase as well as other bacterial enzymes such as phosphatase, peroxidase, and catalase are affected by fluoride [24]. As a result, several studies reported that even low levels of fluoride can affect bacterial growth, the composition of dental plaque, and acid production in vitro [25-28]. Jung and co-workers recently reported that fluoride reduces the proportion of cariogenic bacteria in mixed biofilms from *S. mutans* and *Streptococcus oralis* [29]. However, the results of the present study suggest that, apart from fluoride, other material-related parameters are involved in *S. mutans* biofilm formation on GICs.

Surface roughness and surface free energy are generally regarded as the most important surface properties that affect microbial adhesion to solid surfaces in the oral cavity [30-32]. As it has been observed that differences in substratum surface free energy are at least in parts masked by the presence of an acquired salivary pellicle, surface roughness has been identified as the most important surface parameter for microbial adhesion [30]. Generally, rough surfaces foster the adhesion of microorganisms; however, previous studies identified a

threshold surface roughness at 0.2 µm, suggesting that lower values do not further impact microbial adhesion [33]. In the present study, the surface roughness of the resin-modified, luting, and high-viscosity GICs was markedly higher than the 0.2 um threshold, yet it was not possible to establish a correlation between surface roughness and biofilm formation. While it is clear that the interaction of surface parameters on biofilm formation can be significantly affected by the experimental conditions of a laboratory study, it might also be assumed that surface roughness is a more valid predictor of initial microbial adherence rather than prolonged biofilm formation as performed in the present study. Regarding surface free energy, no significant differences were identified between the materials investigated in the present study, and correlation with biofilm formation data was also poor. These observations support previous results and interpretations [20,34], suggesting that thermodynamic considerations are particularly relevant in the very initial phases of microbial adhesion and determine microbial binding forces rather than adhesion [34].

The low values measured for biofilm formation on the surface of the luting (C) and high-viscosity GIC (D) responded well to the high amounts of dead bacterial cells identified on the surface of these materials observed in the CLSM analyses. These results are supported by previous clinical studies, where biofilms on GICs consisted almost entirely of dead microorganisms [14,15]. After 96 h, the differences observed in biofilm formation between the various materials decreased markedly, yet remained statistically significant; CLSM analyses indicated the presence of a layer of viable bacterial cells on top of the basal layer of predominantly dead bacterial cells adjacent to the substratum surfaces. These observations support the assumption that GICs may inactivate bacterial cells during the early phases of biofilm formation, yet suggest that their efficacy to inhibit biofilm formation decreases with increasing distance from the substratum surface and that the dead bacterial layers adjacent to the surface may serve as sites for subsequent attachment of viable microorganisms. This phenomenon might also be attributed to the observation that – for all materials investigated – there was a general decrease in the release of fluoride with time. This observation suggests rejection of the second study hypothesis and responds to the previously published ``burst effect'' fluoride-releasing materials [35], which could be observed even after the 6 days wash-out period performed prior to the experiments in this study. Nevertheless, the data of this study agree with previous studies from our departments which suggested a relation between biofilm formation and the release of fluoride from experimental RBCs including surface pre-reacted glass ionomer filler particles [22]. In addition to that, the results of the present study showed that changes in the release of fluoride appear to be dependent on the experimental conditions applied. Since the analyses of the release of fluoride from the specimens focused on the release of residual fluoride subsequent to different incubation times and conditions, the data gathered in this study can serve as an indirect description of the kinetics of the release of fluoride. The highest decrease in the release of fluoride was identified for specimens that had been subjected to biofilm formation, which suggests rejection of the third hypothesis of the present study. The different fluoride kinetics identified for specimens that had been subjected to biofilm formation in comparison to those that had been incubated with sterile broth cannot simply be attributed to the acidic environment produced by an acidogenic *S. mutans* biofilm, since low plaque pH conditions that had been experimentally simulated by a constant flow of acids produced an even lower release of residual fluoride after incubation than sterile incubation conditions. This phenomenon might rather be explained by the assumption that the biofilm – and particularly its extracellular matrix – serves as a layer that actively modulates the release of fluoride from the substratum materials. For specimens that had been incubated under acidic conditions merely a slight decrease in the residual release of fluoride was detected with time, which suggests that acidic conditions caused a very high release of fluoride already during the first 48 h of incubation. As it is well-known that fluoride ions have a high bioavailability at low pH conditions, it may be speculated that acidic conditions led to an enhanced burst effect, causing a lower, yet generally more constant release of fluoride over time.

The data of the present study indicate that analyses investigating the release of fluoride from dental materials in the absence of biofilms may not accurately reproduce the clinical

situation, where biofilms are ubiquitous, steadily colonize oral hard surfaces, and actively modulate release kinetics from the surface of bioactive materials. Nevertheless, the authors are aware that the present study has some limitations, including its laboratory character as well as the selection of a monospecies biofilm model. In the oral cavity, biofilms on teeth and restorative materials include a multitude of different bacterial strains embedded into a complex extracellular matrix; thus, it is clear that clinical approaches are the gold standard for the analysis of biofilm formation on restorative materials and that the results of the present study should be corroborated by clinical studies. However, the use of a monospecies biofilm model in this study ensured standardized and reproducible experimental conditions and allows the investigation of several experimental conditions for high-through-output screening. Furthermore, this procedure improves the comparability to other studies on similar topics that used monospecific biofilm models [20-22,36]. Despite of its polymicrobial aetiology, *S. mutans* has been identified as one of the major causative agents of dental caries [37,38], which justifies its selection as test strain in the present study. In contrast to the majority of previous laboratory studies, the model employed in the present study features the simulation of continuous flow conditions [21,39], and included the simulation of salivary pellicle formation [22,36]. Whole saliva had been collected and pooled from different donors in order to minimize interindividual variations in its composition. For storage, the pooled saliva had been frozen until use and was subsequently carefully thawed directly prior to the experiments. While this procedure is regularly employed and well accepted in the literature [40], an impact of freezing and thawing on the properties of the collected saliva cannot be definitely excluded, which might affect pellicle and biofilm formation. However, some researchers demonstrated that the enzymatic activity of different salivary enzymes is only marginally affected by freezing and thawing [41].

In conclusion, and within the limitations of a laboratory study, the results of this research suggest that there is no simple relation between biofilm formation on GICs and their surface properties, while the release of fluoride from GICs contributes to control biofilm formation particularly in its early phases. Interestingly, a bijective relationship was observed for some bioactive materials such as GICs, as they could actively modulate the development of a microbial biofilm which, in turn, was capable of modulating the release of fluoride from the materials surfaces.

<ACK>**Acknowledgements**

Parts of this work were supported by VOCO GmbH, Cuxhaven, Germany.

<REF>References

<BIBL>

[1] G.J. Mount, Glass-ionomer materials, in: G. J. Mount, W. R. Hume, H. C. Ngo, M. S. Wolff (Eds),;1; Preservation and restoration of tooth structure, Sandgate (Qld): Knowledge book and software, cop. 2005. 139-168.

[2] M. Mukai, M. Ikeda, T. Yanagihara, G. Hara, K. Kato, M. Nagagaki, C. Robinson,;1; Fluoride uptake in human dentine from glass-ionomer cement in vivo, Arch. Oral Biol. 38 (1993) 1093-1098.

[3] L. Skartveit, B. Tveit, B. Total, R. Øvrebø, M. Raadal,;1; In vivo fluoride uptake in enamel and dentin fluoride from containing materials, J. Dent. Child. 57 (1990) 97-100.

[4] S.A. Fischman, N. Tinanoff,;1; The effect of acid and fluoride release on the antimicrobial properties of four glassionomers cements, Pediatr. Dent. 16 (1994) 368-370.

[5] L. Seppa, E. Torooa-Saarinen, H. Luoma;1;, Effect of different glassionomer on the acid production and electrolyte metrabolism of Streptococcus mutans, Caries Res. 26 (1992) 434-438.

[6] H. C. Ngo, G. Mount, J. Mc Intyre, J. Tuisuva, R. J. von Dousse,;1; Chemical exchange between glass-ionomer restorations and residual carious dentine in permanent molars: an in vivo study, J. Dent. 34 (2006) 608-613.

[7] K. L. Weerheijm, J. J. de Soete, W. E. van Amerongen, J. de Graaff,;1; The effect of glass-ionomer cement on carious dentin. An in vivo study, Caries Res. 27(5) (1993) 417-423.
[8] M. Behr, C. Kolbeck, R. Lang, S. Hahnel, L. Dirschl, G. Handel,;1; Clinical performance of cements as luting agents for telescopic double crown-retained removable partial and complete overdentures, Int. J. Prosthodont. 22 (2009) 479-487.
[9] M. G. Rasines Alcaraz, A. Veitz-Keenan, P. Sahrmann, P. R. Schmidlin, D. Davis, Z. Iheozor-Ejiofor,;1;Direct composite resin fillings versus amalgam fillings for permanent or adult posterior teeth, <PL>Cochrane</PL> Database Syst. Rev. 31(3) (2014) CD005620.
[10] C. Hannig, F. J. Kupilas, M. Wolkewitz, T. Attin,;1; Validity of decision criteria for replacement of fillings, Schweiz Monatsschr. Zahnmed. 119 (2009) 328–338.
[11] J. W. Nicholson, A. Aggarwal, B. Czarneck, H. Limanowska-Shaw, The rate of change of pH of lactic acid exposed to glass-ionomer dental cements. Biomaterial 21 (2000) 1989-1993.
[12] K. Nakajo, S. Imazato, Y. Takahashi, W. Kiba, S. Ebisu, N. Takahashi,;1; Fluoride released from glass-ionomer cement is responsible to inhibit the acid production of caries-related oral streptococci, Dent. Mater. 25 (2009) 703-708.
[13] N. P. T. Chau, S. Pandit, J. N. Cai, M. H. Lee, J. G. Jeon,;1;Relationship between fluoride release rate and anti-cariogenic biofilm activity of glass ionomer cements, Dent. Mater. 31 (2015) e100-e108.
[14] G. C. Padovani, S. B. Fùcio, G. M. Ambrosano, L. Correr-Sobrinho, R. M. Puppin-Rontani,;1; In situ bacterial accumulation on dental restorative materials. CLSM/COMSTAT analysis, Am. J. Dent. 28 (2015) 3-8.
[15] T. M. Auschill, N. B. Arweiler, M. Brecx, E. Reich, A. Sculean, L. Netuschil,;1; The effect of dental restorative materials on dental biofilm, Eur. J. Oral Sci. 110 (2002) 48-53.
[16] O. T. Al-Naimi, T. Itota, R. S. Hobson, J. F. McCabe,;1; Fluoride release for restorative materials and its effect on biofilm formation in natural saliva, J. Mater. Sci. Mater. Med. 19 (2008) 243-248.
[17] S. Hahnel, G. Mühlbauer, J. Hoffmann, A. Ionescu, R. Bürgers, M. Rosentritt, G. Handel, I. Häberlein,;1; Streptococcus mutans and Streptococcus sobrinus biofilm formation and metabolic activity on dental materials, Acta. Odontol. Scand. 70 (2012) 114-121.
[18] D. K. Owens, R. C. Wendt,;1; Estimation of the surface free energy of polymers, J. Appl. Polym. Sci 13 (1969) 1741-1747.
[19] B. Guggenheim, E. Giertsen, P. Schupbach, S. Shapiro,;1; Validation of an in vitro biofilm model of supragingival plaque, J. Dent. Res. 80 (2001) 363–370.
[20] A. Ionescu, E. Brambilla, D.S. Wastl, F. J. Giessibl, G. Cazzaniga, S. Schneider-Feyrer, S. Hahnel,;1; Influence of matrix and filler fraction on biofilm formation on the surface of experimental resin-based composites, J. Mater. Sci. Mater. Med. 26 (2015) 1-7.
[21] A. Ionescu, E. Wutscher, E. Brambilla, S. Schneider-Feyrer, F. J. Giessibl, S. Hahnel,;1; Influence of surface properties of resin-based composites on in vitro Streptococcus mutans biofilm development, Eur. J. Oral Sci. 120 (2012) 458-465.
[22] S. Hahnel, D. S. Wastl, S. Schneider-Feyrer, F. J. Giessibl, E. Brambilla, G. Cazzaniga, A. Ionescu,;1; Streptococcus mutans biofilm formation and release of fluoride from experimental resin-based composites depending on surface treatment and S-PRG filler fraction, J. Adhes. Dent. 16 (2014) 313-321.
[23] M. F. Hayacibara, O. P. S. Rosa, H. Koo, S. A. Torres, B. Costa, J. A. Cury,;1; Effects of fluoride and aluminum from ionomeric materials on S. mutans biofilm, J. Dent. Res. 82 (2003) 267-271.
[24] I. R. Hamilton,;1; Biochemical effects of fluoride on oral bacteria, J. Dent. Res 69 (1990) 660-667.
[25] C. J. Palenik, M. J. Behnen, J. C. Setcos, C. H. Miller;1;, Inhibition of microbial adherence and growth by various glass ionomers in vitro, Dent. Mater. 8 (1992) 16-20.

[26] L. Seppä, H. Forss, B. Øgaard;1;, The effect of fluoride application on fluoride release and the antibacterial action of glass ionomers, J. Dent. Res. 72 (1993) 1310-1314.
[27] K. H. Friedl, G. Schmalz, K. A. Hiller, M. Shams,;1; Resin-modified glass ionomer cements: fluoride release and influence on Streptococcus mutans growth, Eur. J. Oral. Sci. 105 (1997) 81-85.
[28] K. C. Kan, L. B. Messer, H. H. Messer,;1; Variability in cytotoxicity and fluoride release of resin-modified glass-ionomer cements, J. Dent. Res. 76 (1997) 1502-1507.
[29] J. E. Jung, J. N. Cai, S. D. Cho, K. Y. Song, J. G. Jeon,;1; Influence of fluoride on the bacterial composition of a dual-species biofilm composed of Streptococcus mutans and Streptococcus oralis, Biofouling 32 (2016) 1079-1087.
[30] C. Hannig, M. Hannig,;1; The oral cavity – a key system to understand substratum-dependent bioadhesion on solid surfaces in man, Clin. Oral. Invest. 13 (2009) 123-139.
[31] W. Teughels, N. van Assche, I. Sliepen, M. Quirynen,;1; Effect of material characteristics and/or surface topography on biofilm development, Clin. Oral Impl. Res. 17 Suppl. 2 (2006) 68-81.
[32] G. Cazzaniga, M. Ottobelli, A. Ionescu, F. Garcia-Godoy, E. Brambilla;1;, Surface properties of resin-based composite materials and biofilm formation: a review of the current literature, Am. J. Dent. 28(6) (2015) 311-320.
[33] C. M. Bollen, P. Lambrechts, M. Quirynen;1;, Comparison of surface roughness of oral hard materials to the threshold surface roughness for bacterial plaque retention: a review of the literature, Dent. Mater. 13 (1997) 258-269.
[34] H. J. Busscher, M. Rinastiti, W. Siswomihardjo, H. C. Van der Mei,;1; Biofilm formation on dental restorative and implant materials, J. Dent. Res. 89 (2010) 657–665.
[35] L. Forsten,;1; Fluoride release and uptake by glass-ionomers and related materials and its clinical effect, Biomaterials 19 (1998) 503-508.
[36] A.C. Ionescu, E. Brambilla, A. Travan, E. Marsich, I. Donati, P. Gobbi, G. Turco, R. Di Lenarda, M. Cadenaro, S. Paoletti, L. Breschi.;1; Silver-polysaccharide antimicrobial nanocomposite coating for methacrylic surfaces reduces Streptococcus mutans biofilm formation in vitro, J. Dent. 43 (2015b) 1483-1490.
[37] J. D. De Stoppelaar, J. van Houte, O. Backer Dirks,;1; The relationship between extracellular polysaccharide-producing streptococci and smooth surface caries in 13-year-old children, Caries Res. 3 (1990) 190-199.
[38] S.D. Forssten, M. Bjorklund, A.C. Ouwehand,;1; Streptococcus mutans, caries and simulation models, Nutrients 2 (2010) 290–298.
[39] C.H. Sissons,;1; Artificial dental plaque biofilm model systems, Adv. Dent. Res. 11 (1997) 110-126.
[40] C. A. Francis, M. P. Hector, G. B. Proctor,;1; Precipitation of specific proteins by freeze-thawing of human saliva, Arch. Oral. Biol. 45 (2000) 606-606.
[41] C. J. Williams, F. W. Kraus;1;, Sterilization and storage of saliva, J. Dent. Res. 42 (1963) 1416-1428.

</BIBL>

Figures

<Figure>Figure 1. Surface roughness of the materials investigated at baseline. Means ± 1 standard error are indicated.

<Figure>Figure 2. Surface free energy (total; disperse and polar contributions) at baseline; means ± 1 standard error are indicated.

<Figure>Figure 3. Relative absorbance correlating with *Streptococcus mutans* biofilm formation after either 48 h or 96 h. Means ± 1 standard error are indicated; different superscript letters indicate significant differences between groups ($p<.05$).

<Figure>Figure 4. Fluoride release results after biofilm formation, incubation with sterile broth, or acid for either 48 h or 96 h. Means ±1 standard error are indicated; different superscript letters indicate significant differences between groups ($p<.05$).

<Figure>Figure 5. Series of 750 x 750 µm CLSM reconstructions of *Streptococcus mutans* biofilms after 48 h. Viable bacterial cells are displayed in green, whereas dead cells are displayed in red. The letter code responds to the substratum material.

<Figure>Figure 6. Series of 750 x 750 µm CLSM reconstructions of *Streptococcus mutans* biofilms after 96 h. Viable bacterial cells are displayed in green, whereas dead cells are displayed in red. The letter code corresponds to the substratum material.

<Figure>Figure 7. Series of 2000x magnification SEM micrographs of *Streptococcus mutans* biofilms after 48 h. The letter code corresponds to the substratum material.

<Figure>Figure 8. Series of 2000x magnification SEM micrographs of *Streptococcus mutans* biofilms after 96 h. The letter code corresponds to the substratum material.

<Table>Table 1. Surface composition (wt%) of the materials investigated at baseline as determined by EDS analyses.

	C	**F**	**Al**	**Si**	**P**	**Na**	**K**	**Ba**	**Fe**	**Ca**
A	57.56	**8.53**	12.07	16.26	3.84	1.11	0.63			
B	62.31		6.86	24.99				5.72	0.12	
C	52.48	**9.16**	13.69	17.86	4.73	1.43	0.65			
D	42.47	**10.48**	16.88	23.99	3.00	1.5	0.74			0.94
E	15.54		6.82	44.14				33.5		
F	5.06				40.10	1.64				53.20

<Table>Table 2. Fluoride surface content (wt%) of the materials investigated after biofilm formation, incubation with sterile broth, or acid as assessed by EDS analysis.

	biofilm		**sterile broth**		**acid**	
	48 h	96 h	48 h	96 h	48 h	96 h
A	2.51	1.95	2.67	3.61	0.70	0.60
B	0.71	---	0.94	1.47	---	---
C	1.55	2.26	3.89	1.5	2.31	2.08
D	2.55	3.25	4.83	3.93	1.61	1.50

E	---	---	---	---	---	---
F	---	---	---	---	---	---

TDENDOFDOCTD